ELSEVIER

Journal of Organometallic Chemistry 577 (1999) 103–112

Journal of Organometallic Chemistry

Titanium-catalyzed head-to-tail dimerization of *tert*-butylacetylene. Crystal structures of $[(C_5HMe_4)_2Ti(\mu\text{-}H)_2Mg(THF)(\mu\text{-}Cl)]_2$ (THF-tetrahydrofuran) and $(C_5HMe_4)_2TiOCMe_3$

Michal Horáček [a], Ivana Císařová [b], Jiří Čejka [a], Jindřich Karban [a], Lidmila Petrusová [a], Karel Mach [a,*]

[a] *J. Heyrovský Institute of Physical Chemistry, Academy of Sciences of the Czech Republic, Dolejškova 3, 182 23 Prague 8, Czech Republic*
[b] *Department of Inorganic Chemistry, Charles University, 128 40 Prague 2, Czech Republic*

Received 4 September 1998; received in revised form 5 October 1998

Abstract

tert-Butylacetylene (TBUA) is readily dimerized exclusively to 2,4-di-*tert*-butyl-1-buten-3-yne, head-to-tail dimer (HTTD), in the presence of the $(\eta^5\text{-}C_5HMe_4)_2TiCl_2/Mg/THF$ system. The ESR investigation revealed the formation of Ti–Mg hydride complexes $[(\eta^5\text{-}C_5HMe_4)_2Ti(\mu\text{-}H)_2Mg(THF)(\mu\text{-}Cl)]_2$ (**2**) and $[(\eta^5\text{-}C_5HMe_4)_2Ti(\mu\text{-}H)_2]_2Mg$ (**3**) in the absence of TBUA and a tweezer-type complex, probably $[(\eta^5\text{-}C_5HMe_4)_2Ti(\eta^1\text{-}C{\equiv}CCMe_3)_2]^-$ $[Mg(THF)Cl]^+$ (**4**) in its presence. The catalytic system as well as complexes **2**–**4** were deactivated by presumably *tert*-butanol contained in TBUA to give $(\eta^5\text{-}C_5HMe_4)_2TiOCMe_3$ (**5**). Purification of TBUA improved the turnover by up to 8.8×10^3 mol TBUA per 1 mol Ti using complex **3** as a catalyst, however, complex **5** remained the only observable product of deactivation. The crystal structures of **2** and **5** were determined by X-ray diffraction analysis.

Keywords: *tert*-Butylacetylene; Dimerization; Electron spin resonance; Bis(tetramethylcyclopentadienyl)titanium(III) hydride catalyst; Bis(tetramethylcyclopentadienyl)titanium(III) *tert*-butoxide; Crystal structures

1. Introduction

Linear dimerization of terminal acetylenes to exclusively head-to-tail dimers catalyzed by permethyltitanocene catalysts falls into a class of enzymatically selective reactions [1]. The $(C_5Me_5)_2TiCl_2/2$ *i*-PrMgCl (*i*-Pr = isopropyl) system in diethyl ether was shown to dimerize all terminal acetylenes except those containing an electron donor atom in their substituent and *tert*-butylacetylene (TBUA) [2]. We have recently found that the catalyst activity increases with increasing molar Mg/Ti ratio up to about ten and vanishes when the pentamethyl-substituted cyclopentadienyl ligands are replaced by the tetramethyl—or less substituted cyclopentadienyl ligands [3]. A puzzling inertness of TBUA has been attributed to steric congestion in a transient catalytic complex [2]. This assumption seemed to be justified by catalytic experiments performed with permethylmetallocene carbyls of rare-earth elements Sc [4], Y [5], Y, La, and Ce [6,7]; only those having large ionic radii (La, Ce) catalyzed the head-to-tail dimerization of TBUA. In the transition metal series, a cationic permethylzirconocene complex has also been found to catalyze the head-to-tail dimerizaton of TBUA [8]. This was attributed to steric relief resulting from a larger ionic radii of La, Ce and Zr compared to Ti [9].

Here we report the selective head-to-tail dimerization of TBUA catalyzed by the $(C_5HMe_4)_2TiCl_2/Mg/THF$ system and by individual complexes contained in the system, the ESR study of the reacting systems, and crystal structures of a Ti–Mg hydride-bridged complex,

* Corresponding author. Tel.: +42-2-858-5367; fax: +42-2-858-2307.

0022-328X/99/$ - see front matter
PII: S0022-328X(98)01031-6

which is the catalyst precursor, and a product of deactivation.

2. Experimental details

2.1. General data and methods

Preparations of the $(\eta^5\text{-}C_5HMe_4)_2TiCl_2$/Mg/THF systems, isolation of individual complexes, their handling and spectroscopic measurements were performed under vacuum. *tert*-Butylacetylene was purified, stored and dosed on a vacuum line. All-sealed glass devices equipped with breakable seals, an EPR sample tube and a pair of quartz cells ($d = 1.0$ and 10 mm; Hellma) were used for measurements of ESR and UV–NIR spectra. These devices were also used as reaction vessels for the catalytic experiments. ESR spectra were recorded on an ERS-220 spectrometer (Centre for Production of Scientific Instruments, Academy of Sciences of GDR, Berlin, Germany) equipped with a magnet controlling and data acquisition CU1 unit (Magnettech, Berlin, Germany) in the X-band. The g-values were determined using an Mn^{2+} ($M_I = -1/2$ line) standard at $g = 1.9860$. Concentrations of the paramagnetic compounds were estimated from integrated first derivative spectra. An STT-3 variable temperature unit was used for the measurement in the range -140 to $+20$°C. UV–NIR spectra were measured in the range 270–2000 nm on a Varian Cary 17D spectrometer. IR were registered on a Specord 75 IR (Carl Zeiss, Jena, Germany).

Mass spectra of deactivated catalysts in the solid state were measured on a VG 7070E spectrometer at 70 eV (only important mass peaks and peaks of intensity $\geq 5\%$ are reported) using a direct inlet. Samples in capillaries were opened and inserted into the direct inlet under argon. GC–MS analyses were carried out on a Hewlett Packard gas chromatograph (5890 series II) equipped with a capillary column SPB-1 (length 30 m; Supelco) and a mass spectrometric detector (5971 A). The quantitative GC determination of head-to-tail dimer of TBUA (HTTD) in reaction mixtures was carried out on a CHROM 5 gas chromatograph (Laboratory Instruments, Prague, Czech Republic) using *n*-decane as a standard. ^{1}H- and ^{13}C-NMR spectra of HTTD were recorded in $CDCl_3$ solutions on a Varian VXR-400 spectrometer (400 and 100 MHz, respectively) in $CDCl_3$. Chemical shifts (given in the δ scale) were referenced to TMS.

2.2. Chemicals

The solvents THF, diethyl ether, hexane, and toluene were purified by conventional methods, dried by refluxing over $LiAlH_4$, and stored as solutions of dimeric titanocene $(\mu\text{-}\eta^5\text{:}\eta^5\text{-}C_{10}H_8)[(\eta^5\text{-}C_5H_5)Ti(\mu\text{-}H)]_2$ [10]. TBUA (Aldrich; 98%) was degassed on a vacuum line and distilled onto dimeric titanocene. The obtained solution was warmed to 50°C. If it turned red, TBUA was distilled onto another portion of dimeric titanocene. This purification operation was repeated (typically 2–3 times) until the solution turned brown. Finally, TBUA was distilled into a storage ampoule containing solid $[(C_5Me_5)_2Ti(\mu\text{-}H)_2]_2Mg$ [11]. Bis(tetramethylcyclopentadienyl)titanium dichloride $(\eta^5\text{-}C_5HMe_4)_2TiCl_2$ (**1**) was obtained as described elsewhere [12]. Magnesium (for Grignard reagents; Aldrich) was used as such. Crystalline $[(C_5HMe_4)_2Ti(\mu\text{-}H)_2]_2Mg$ (**3**) is an authentic sample described in Ref. [13]. Tweezer complexes $[(\eta^5\text{-}C_5HMe_4)_2Ti(\eta^1\text{-}C{\equiv}CSiMe_3)_2]^-$ $[Mg(THF)Cl]^+$ (**4′**) and $[(\eta^5\text{-}C_5Me_5)_2Ti(\eta^1\text{-}C{\equiv}CSiMe_3)_2]^-$ $[Mg(THF)Cl]^+$ (**4″**) (both 0.05 mmol in 5 ml) are authentic samples described in Ref. [14].

2.3. The $(C_5HMe_4)_2TiCl_2$/Mg/THF catalytic system and dimerization of TBUA

A typical catalyst was obtained from **1** (0.361 g, 1.0 mmol) and Mg (0.243 g, 10.0 mmol) in 20 ml of THF by warming to 60°C for typically 2 h. The reaction time may differ in dependence upon the length of induction period by ca. 1 h. The initial red colour of the solution turns via an intermediate blue color typical of $(\eta^5\text{-}C_5HMe_4)_2TiCl$ to dark brown. This solution was divided into 2 ml portions each portion containing 0.1 mmol of Ti. These were transferred to the reaction vessels equipped with an EPR tube and quartz cells for UV–NIR measurements and the measured volume of liquid TBUA was distilled in on a vacuum line. The reaction mixture was cooled by liquid nitrogen and the reaction vessel was sealed off and immersed into a water bath thermostatted to 60°C. The course of TBUA consumption was followed by the decrease in intensity of the absorption band at 1530 nm ($2 \times \nu$(C–H) of TBUA). The measurement of kinetics of the dimerization was not attempted as it was impossible to keep the temperature constant during the ESR and UV–NIR measurements. Another portion of TBUA was added on a vacuum line when all TBUA was consumed. When TBUA was no longer consumed within 4 h at 60°C all volatiles were distilled off at ambient temperature into an ampoule cooled by liquid nitrogen. These volatiles were qualitatively analyzed by GC–MS, quantitatively by GC using *n*-decane as an internal standard and finally the dimer was isolated by fractional distillation. TBUA purified by dimeric titanocene gave turnover numbers TBUA mol/Ti mol (TON) in the range of 450–550.

2,4-di-*tert*-Butyl-1-buten-3-yne (HTTD). MS (GC–MS, m/z (%)): 164 ($M^{\cdot+}$, 9), 149 (18), 121 (6), 108 (16), 107 (14), 105 (10), 93 (42), 92 (5), 91 (33), 79 (12), 77

(22), 65 (15), 63 (7), 58 (5), 57 (100), 55 (7), 53 (13), 52 (6), 51 (16), 50 (5), 43 (6), 41 (58), 39 (33), 29 (26), 28 (5), 27 (15). IR (neat) (cm^{-1}): 3096(m), 2958(vs), 2920(sh), 2897(vs), 2857(vs), 2207(m), 1789(w), 1604(s), 1590(sh), 1542(vw), 1475(s), 1458(s), 1380(s), 1359(s), 1308(s), 1296(m), 1250(s), 1202(s), 1176(s), 1025(w), 994(w), 925(vw), 892(vs), 875(m), 817(w), 715(vw), 649(m), 567(vw), 535(w), 515(m), 460(vw). ^{1}H-NMR ($CDCl_3$): δ 1.337 (9H, s, *t*-Bu at C-2), 1.478 (9H, s, *t*-Bu at C-4), 5.344 (1H, d, $J = 1.6$ Hz), 5.394 (1H, d, $J = 1.6$ Hz). ^{13}C-NMR ($CDCl_3$): 27.92 (s, *t*-Bu at C-4), 28.99 (q, 3C, *t*-Bu at C-2), 31.08 (q, 3C, *t*-Bu at C-4), 36.03 (s, *t*-Bu at C-2), 78.75 (s, C-3), 99.05 (s, C-4), 115.70 (t, C-1), 142.04 (s, C-2).

The assignment is based on HETCOR, long-range HETCOR, and proton-coupled ^{13}C-NMR. Exomethylene protons are long-range coupled to a quaternary carbon (δ 36.03 ppm) carrying three methyls and to sp-hybridized carbon C-3 (δ 78.75 ppm). The respective *t*-Bu protons are coupled to the sp^2-type carbon C-2 (δ 142.04 ppm). Protons of the *t*-Bu group attached to C-4 exhibit a long-range couplings to a quaternary carbon at δ 27.92 ppm and to the second sp-type carbon C-4 (δ 99.05 ppm) (cf. [7]).

2.4. Synthesis of $[(\eta^5\text{-}C_5HMe_4)_2Ti(\mu\text{-}H)_2Mg(THF)(\mu\text{-}Cl)]_2$ (2)

A mixture of **1** (1.445 g, 4 mmol), Mg (1.0 g, 41 mmol) and THF (50 ml) was heated to 60°C for 4 h. The colour changed from bright red to blue, purple and final brown. THF was evaporated, and a brown residue was extracted by hexane (20 ml) until the extract was colourless. ESR spectrum of the red–brown solution revealed the presence of a compound characterized by a single line at $g = 1.992$ with $\Delta H = 0.6$ mT and a trace of $(\eta^5\text{-}C_5HMe_4)_2TiCl$ (cf. [15]). A pale-blue residue was repeatedly extracted by toluene (100 ml) until a nearly colourless crystalline residue of presumably $MgCl_2$ remained. The extract was evaporated and the residue was extracted once more. As a result, another small amount of a white solid was separated from a pale purple–blue solution. Upon cooling overnight to 0°C blue fine needles of **2** grew out, forming rich aggregates. Mother liquor was concentrated to a half volume and afforded another crop of crystals. This mother liquor was not worked up any further since its ESR spectrum showed the presence of the $[(\eta^5\text{-}C_5HMe_4)_2Ti(\mu\text{-}H)_2]_2Mg$ (**3**) complex. In the frozen toluene glass, complex **3** displays the spectrum of an electronic triplet state of axial symmetry ($g = 1.9907$, $D = 0.01327$ cm^{-1}, $E = 0$) [13], well discernible from the spectrum of **2**. The structure of **2** was determined by X-ray single crystal analysis (vide infra). Yield 1.1 g (1.3 mmol, 65%). MS (direct inlet, 70 eV, 120–220°C): evolution of THF; no other volatile products or fragments. UV–NIR (toluene) (nm): 500 > 560(sh, absorption extends to 900 nm). ESR (toluene, 22°C): $g = 1.9914$, a_H (triplet 1:2:1) = 0.7 mT, a_H (odd multiplets) = 0.1 mT; (toluene, −140°C): $g_1 = 2.0013$, $g_2 = 1.9917$, $g_3 = 1.9836$, $g_{av} = 1.9922$, $a_1 = 0$, $a_2 = 0.6$ mT, $a_3 = 1.0$ mT. IR (KBr) (cm^{-1}): 3095(w), 2903(vs), 2722(w), 1449(m), 1381(m), 1292(s) (*v* Ti–H), 1138(m), 1026(s) (THF), 976(w), 936(w), 878(m), 826(m), 781(m), 660(m), 422(m).

2.5. Catalysis by hydride complexes 2 and 3 and tweezer complexes 4′ and 4″

Crystals of **2** (10 mg, 0.018 mmol) were dissolved in 2.0 ml of THF (5 ml) and 4.5 ml of TBUA (purified finally by $[(C_5Me_5)_2Ti(\mu\text{-}H)_2]_2Mg$ [13]) was added. After heating to 60°C for 18 h ca. 95% of TBUA was consumed. This corresponds to TON ca. 2×10^3. Toluene solutions of tweezer complexes $(\eta^5\text{-}C_5HMe_4)_2Ti(\eta^1\text{-}C{\equiv}CSiMe_3)_2]^-$ $[MgCl(THF)]^+$ (**4′**) or $(\eta^5\text{-}C_5Me_5)_2Ti(\eta^1\text{-}C{\equiv}CSiMe_3)_2]^-$ $[MgCl(THF)]^+$ (**4″**) (both 0.05 mmol in 5 ml) were also used as catalysts in the same experimental arrangement. Complex **4′** consumed 6.1 ml of TBUA (TON ca. 1×10^3) while **4″** was inactive. Crystals of **3** (22 mg, 0.036 mmol) were added to 8 ml of TBUA and this mixture was heated to 60°C. TBUA was consumed after ca. 45 min while not all crystals dissolved. HTTD was distilled off on a vacuum line and a new portion of TBUA was distilled in. This was repeated until total consumption of TBUA was 39 ml (TON ca. 8.8×10^3).

2.6. Isolation of $(\eta^5\text{-}C_5HMe_4)_2TiOCMe_3$ (5)

A commercial TBUA (Aldrich, 25 ml) was degassed and distilled to crystalline $[(\eta^5\text{-}C_5HMe_4)_2Ti(\mu\text{-}H)_2]_2Mg$ (0.10 g, 0.16 mmol). A bubbling occurred within the crystals and continued until the crystals dissolved. The color of the solution turned brown. All volatiles were distilled off and analyzed by gas chromatography: a portion of TBUA was dimerized to head-to-tail dimer (ca. 2–4 ml, 16–32 mmol). The residue was extracted by a minimum amount of hexane. The extract was evaporated and extracted again by the same hexane in order to remove traces of a white solid. Crystallization at low temperature afforded greenish–brown crystals of **5** which were used for X-ray single crystal analysis and ESR measurements in toluene solution and glass. Yield 50 mg (85%). EI MS (direct inlet, 70 eV, 70°C): 364 (10), 363 ($M^{+\cdot}$, 34), 308 (5), 307 (19), 291 (14), 290 (39), 289 (100), 288 (18), 287 (24), 285 (8), 242 (8), 226 (20), 225 (8), 186 (32), 185 (22), 184 (13), 183 (8), 181 (10), 169 (11), 168 (43), 167 (22), 166 (25), 165 (9), 164 (12), 163 (6), 145 (8), 105 (7), 64 (18), 57 (8), 41 (7). ESR (toluene, 22°C): $g = 1.979$, $\Delta H = 0.4$ mT, $a_{Ti} = 0.9$ mT; (toluene, −140°C): $g_1 = 2.001$, $g_2 = 1.982$, $g_3 = 1.955$, $g_{av} = 1.979$. IR (KBr) (cm^{-1}): 3066(vw), 2959(s),

Table 1
Crystallographic and structure refinement data for **2** and **5**

	2	**5**
Crystal data		
Chemical formula	$C_{44}H_{72}Cl_2Mg_2O_2Ti_2$	$C_{22}H_{35}OTi$
Molecular weight	848.33	363.40
Crystal system	Monoclinic	Monoclinic
Space group	$P2_1/n$ (no. 14)	$P2_1/c$ (no. 14)
a (Å)	8.8050(10)	15.504(2)
b (Å)	10.1870(10)	8.240(4)
c (Å)	26.4450(10)	16.542(3)
β (°)	97.450(10)	91.110(10)
V (A^3)	2352.0(4)	2112.9(11)
Z	4	4
$D_{calc.}$ (g cm^{-3})	1.198	1.142
μ(Mo–K_α) (mm^{-1})	0.512	0.410
F(000)	908	788
Crystal colour	Blue	Brown
Crystal size (mm)	$0.57 \times 0.50 \times 0.43$	$0.57 \times 0.35 \times 0.28$
Data collection and refinement		
Temperature (K)	293(2)	150(0.1)
$\theta_{min.}$, $\theta_{max.}$ (°)	1.55, 24.97	1.31, 23.98
Range of indices (h, k, l)	$0 \rightarrow 10$, $0 \rightarrow 12$, $-31 \rightarrow 31$	$0 \rightarrow 17$, $0 \rightarrow 9$, $-18 \rightarrow 18$
Reflections collected	4400	3437
Independent reflections	4124 [$R_{int} = 0.0233$]	3311 [$R_{int} = 0.0134$]
Data, restraints, parameters	4124, 0, 243	3311, 0, 357
Goodness-of-fit on F^2	1.020	1.039
$R1$, $wR2$ [$I > 2\sigma(I)$]	0.0495, 0.1209	0.0318, 0.0848
$R1$, $wR2$ (all data)	0.1105, 0.1515	0.0445, 0.0913
Max. and min. residual density (e A^{-3})	0.343; −0.343	0.227; −0.259

2903(vs), 2853(s), 1442(s), 1378(s), 1353(m), 1329(w), 1188(s), 1078(w), 1020(m), 1002(s), 906(w), 827(sh), 812(vs), 780(s), 733(vs), 700(s), 637(m), 620(m), 574(s), 540(w). UV–NIR (hexane) (nm): $390 \gg 620$ (sh) > 1170.

2.7. X-ray structure determination of **2** and **5**

Fragments of dark blue needle crystals of **2** and brown crystals of **5** were mounted into Lindenmann glass capillaries under purified nitrogen in a glovebox (mBraun) and were closed with a sealing wax. Diffraction data were collected on a Enraf-Nonius CAD-4 diffractometer (graphite monochromated Mo–K_α radiation, λ 0.71069 Å) at 293(2) K for **2** and at 150(0.1) K for **5**. A cryostream cooler (Oxford Cryosystem) was used in the latter case. The low-temperature measurement was necessary to decrease large temperature factors of methyl carbon atoms of the *tert*-butoxy group. The structures were solved by direct methods (SHELXS97) [16]. The refinement was done with full matrix least-squares methods based on F^2 applying variance-based weighting schemes (SHELXL97) [17]. For **2** all non-hydrogen atoms were refined anisotropically. Bridging hydrogen atoms were located on a difference Fourier map and refined isotropically. All other hydrogen atoms were included in calculated positions. For **5**, non-hydrogen atoms were refined anisotropically. All hydrogen atoms were located on a difference Fourier map and refined isotropically. Details of data collection and refinement are given in Table 1.

3. Results and discussion

TBUA is at least 99.9% selectively converted to the head-to-tail dimer (HTTD), 2,4-di-*tert*-butyl-1-buten-3-yne, by the $(C_5HMe_4)_2TiCl_2$/Mg/THF system (Scheme 1). The turnover numbers TBUA/Ti (mol)/(mol) (TON) 450–550 were obtained with TBUA purified by dimeric titanocene only. The conversion was completed after ca. 20 h. Further purification of TBUA by treatment with $[(C_5Me_5)_2Ti(\mu\text{-}H)_2]_2Mg$ considerably decreased the content of an impurity. This TBUA was used for catalytic experiments with pure complexes **2**, **3**, **4′**, and **4″** in which much higher TONs were achieved (vide infra). The purity of TBUA had however, no effect on

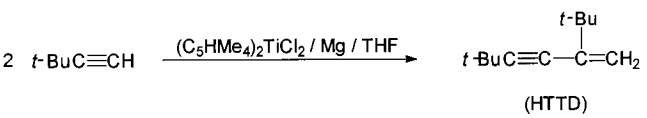

Scheme 1.

the selectivity of the dimerization, which always afforded practically pure HTTD.

3.1. The composition of the catalytic system

The reduction of **1** by magnesium in THF is easily followed by ESR spectroscopy as a great majority of products are compounds of Ti(III). After an induction period, the reduction of **1** at 60°C proceeds rapidly via the intermediate formation of blue monomeric $(C_5HMe_4)_2TiCl$ which does not coordinate THF [15]. The colour then turns brown and the system contains mainly three products. A minor, red component characterized by ESR signal at $g = 1.992$ ($\Delta H = 0.6$ mT) can be readily extracted by hexane. Its structure is unknown and its eventual role in the TBUA dimerization is not important as the selectivity of dimerization was not affected by its presence or absence. The products insoluble in hexane are titanocene hydride–magnesium hydride complexes. They are easily recognized by ESR spectroscopy. The main product was the dimeric complex $[(\eta^5\text{-}C_5HMe_4)_2Ti(\mu\text{-}H)_2Mg(THF)(\mu\text{-}Cl)]_2$ (**2**) whose ESR spectrum does not reflect the dimeric structure. Interaction of the Ti(III) d^1 electron with two bridging hydrides ($a_H = 0.7$ mT) and a superhyperfine splitting with protons of the C_5HMe_4 ligands ($a_H = 0.1$ mT) gives three odd multiplets in the ca. 1:2:1 intensity ratio at $g = 1.991$ (Fig. 1(a)). This spectrum is undistinguishable from that of the analogous complex $[(\eta^5\text{-}C_5HMe_4)_2Ti(\mu\text{-}H)_2Mg(OEt_2)(\mu\text{-}Cl)]_2$ obtained in the $(C_5HMe_4)_2TiCl_2/i\text{-}PrMgCl/OEt_2$ system [18]. The crystal structure of **2** revealed the presence of coordinated THF and a somewhat different overall structure in the solid state (vide infra). The minor product was identified by ESR measurement of the catalytic system transferred to toluene solution and measured in glassy state. Its spectrum of the electronic triplet state of axial symmetry was identical with that of $[(C_5HMe_4)_2Ti(\mu\text{-}H)_2]_2Mg$ (**3**) [13]. The crystalline compound **2** isolated from this system and crystals of **3** (authentic sample from Ref. [13]) showed a high activity and selectivity in the formation of HTTD (vide infra).

3.2. The nature of impurity in TBUA and its effect on TON

Investigation of intermediate complexes arising from the reaction of **2** or **3** with TBUA and of the products of deactivation was, unfortunately, hampered by an impurity in commercial *t*BuA.

The impurity was apparently *tert*-butanol as the product of deactivation in all the catalysts mentioned except the parent system was $(\eta^5\text{-}C_5HMe_4)_2TiOCMe_3$ (**5**); its ESR spectrum ($g = 1.978$, $\Delta H = 0.4$ mT, $a_{Ti} = 0.9$ mT) was observable in all the investigated catalytic systems. The ESR spectrum was very similar to that of

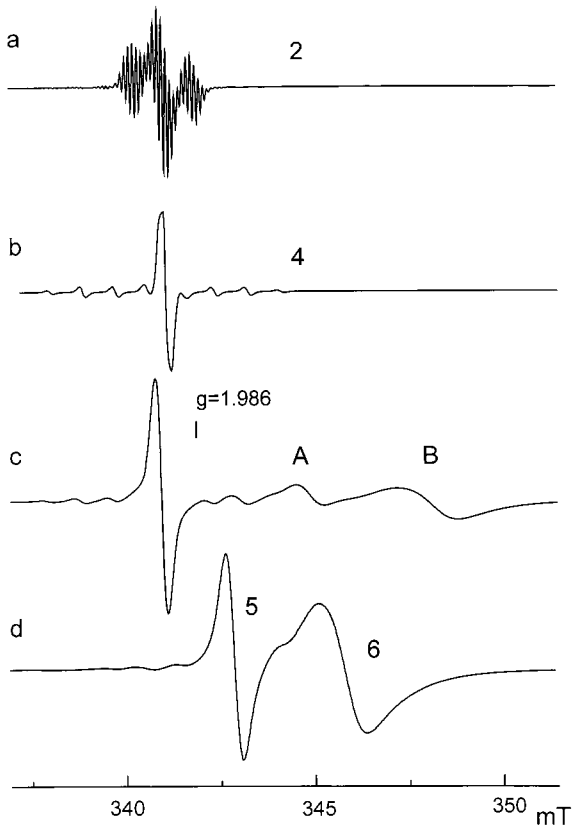

Fig. 1. ESR spectra of the $(C_5HMe_4)_2TiCl_2/Mg/THF$ system before addition of TBUA (a) and after addition of TBUA (b)–(d). Conditions: (a) extremely diluted, measured at −15°C, modulation amplitude 0.01 mT; (b) very diluted, at 22°C, modulation amplitude 0.1 mT; (c) and (d) arbitrary diluted, at 22°C, modulation amplitude 0.1 mT.

$(\eta^5\text{-}C_5Me_5)_2TiOCMe_3$ [19] or $(\eta^5\text{-}C_5Me_5)_2TiOMe$ [20] and its electronic spectrum resembled that of $(\eta^5\text{-}C_5Me_5)_2TiOMe$ [20]. Nevertheless, the chemical composition and the structure of **5** was determined by X-ray diffraction analysis of crystals isolated from the reaction of commercial TBUA with complex **3**. The formation of **5** strongly corroborates the presence of *tert*-butanol in TBUA, however, the direct evidence e.g. from GC–MS was not obtained because the retention time of *tert*-butanol was only slightly longer than that of TBUA and its fragment ions coincide with those of TBUA or the instrument background ions. Chemical elimination of *tert*-butanol is difficult because it seems to react with strong bases only slightly faster than TBUA. Application of dimeric titanocene is profitable as the red di-(μ-*t*-butoxy) compound was formed preferentially in early stages of the purification. At lower concentrations of *tert*-butanol, brown mono-μ-*tert*-butylacetylide prevails (for analogous reaction with (trimethylsilyl)acetylene see Ref. [21]). The TBUA purification by the above catalytic system or by hydride complexes **2** or **3** is not economical as all of them induce a competitive dimerization of TBUA. So far the

most effective was the treatment of the TBUA prepurified by dimeric titanocene with solid $[(C_5Me_5)_2Ti(\mu\text{-}H)_2]_2Mg$ [13], which does not dimerize TBUA. Such TBUA was used for catalytic experiments with pure complexes **2, 3**, **4′** and **4″**. The TONs are increasing in the order **4′** TON $1.0 \times 10^3 <$ **2** TON $2.0 \times 10^3 <$ **3** TON 8.8×10^3. Compound **4″** was inactive. The above given TONs may reflect the capacity of compounds to bind *tert*-butanol. Surprisingly, the only observable product of deactivation in the most effective system with **3** was again compound **5**. Since it is difficult to imagine its formation from oxygen of glass surface we have to accept that some concentration of the impurity persists in the solution of $[(C_5Me_5)_2Ti(\mu\text{-}H)_2]_2Mg$ in TBUA. It also implies that unforeseeably higher TONs would be achievable in pure TBUA. The comparison with activities of other highly selective systems [6–8,22] is difficult as all of them are based on the measurement in NMR tubes where a maximum ratio of TBUA to catalyst of about 500 [22] was used.

3.3. ESR study of dimerizing systems

The ESR spectra of the $(C_5HMe_4)_2TiCl_2$/Mg/THF system in toluene solution after addition of TBUA indicates a limited number of species. The main component **2** was rapidly transformed into a tweezer complex which is characterized by a single narrow line at $g = 1.991$ ($\Delta H = 0.32$ mT) flanked by ca. 20 times weaker multiplets due to ^{49}Ti and ^{47}Ti isotopes ($a_{Ti} = 0.85$ mT) (Fig. 1(a, b)). ESR spectra of this appearance are typical of anionic titanocene(Ti(III) diacetylide tweezer complexes which contain a metal cation embedded between the anionic acetylide arms [14,23,24] (for numerous Ti(IV) tweezer complexes see recent works [25]). In the present case, the cation is assumed to be $[Mg(THF)Cl]^+$, as found e.g. in the X-ray crystal structure of $[(\eta^5\text{-}C_5HMe_4)_2Ti(\eta^1\text{-}C{\equiv}CSiMe_3)_2]^-$ $[Mg(THF)Cl]^+$ (**4′**) [14]. A number of complexes of this type with various substituents on acetylide ligands was identified by ESR spectra in the $(C_5Me_5)_2TiCl_2$/Mg/OEt_2/RC≡CH systems [3]. A superhyperfine splitting is observed in cases where the α-carbon of R bears protons and the sum of equivalent protons in both arms determines the splitting multiplicity. Such protons are absent in the *tert*-butyl substituent and thus a sharp central single line and other parameters are compatible with the formula $[(\eta^5\text{-}C_5HMe_4)_2Ti(\eta^1\text{-}C{\equiv}CCMe_3)_2]^-$ $[Mg(THF)Cl]^+$ (**4**) (see Fig. 1(b)). The ESR spectrum of **4** is then diminishing and new signals at $g = 1.979$ ($\Delta H = 0.45$ mT), $g = 1.968$ ($\Delta H = 0.58$ mT) and $g = 1.951$ ($\Delta H = 1.58$ mT) grow in intensity (Fig. 1(c)). The first of them is identical with the signal of **5**. The other signals (denoted **A** and **B**) are not assigned, however, they occur inherently in all the catalytically active systems. As concerns signal **B**, we believe that it belongs to monomeric titanocene *tert*-butylacetylide, $(\eta^5\text{-}C_5HMe_4)_2Ti(\eta^1\text{-}C{\equiv}CCMe_3)$. The reason is that its g-value can be expected to be low (cf. $(\eta^5\text{-}C_5HMe_4)_2TiMe$, $g = 1.9637$ $\Delta H = 1.4$ mT [26] and $(C_5Me_5)_2TiMe$, $g = 1.956$ and $(C_5Me_5)_2TiC{\equiv}CMe$, $g = 1.941$ [27]) and the dissociation of **4** into Ti and Mg components has to occur before a final deactivation product is produced. Finally, all the ESR signals disappear, giving rise to the signal of $(\eta^5\text{-}C_5HMe_4)_2TiCl$ (**6**) at $g = 1.963$ ($\Delta H = 1.24$ mT) (cf. [15]). Pure complex **2** affords all the above mentioned species, however, its deactivation ends up with a mixture of **5** and **6** (Fig. 1(d)). Complex **4′** used as a catalyst in toluene gives the same results as complex **2** after its conversion to **4**. Compound **3** in TBUA dissolved slowly even at 60°C; the solution was obtained only after TON ca. 3×10^3 was reached. A tweezer complex was formed only in low concentration and its ESR signal was broad, ca. $\Delta H = 0.45$ mT. These data were drawn from satellite ^{47,49}Ti multiplets since the tweezer central line was overlapped by the signal of **3** at $g = 1.991$. Other observed signals were identical with those described above (cf. Fig. 1(c)). The product of deactivation was only **5** and the intensity of its ESR spectrum roughly corresponded to overall titanium concentration.

The chemistry involved can be expressed by reactions (1)–(3). The conversion of **2** to **4** can be straightforward:

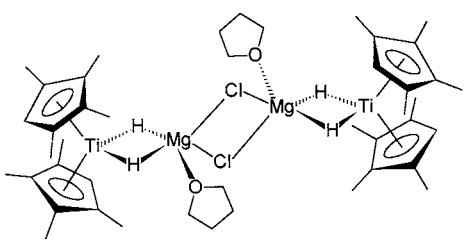

2

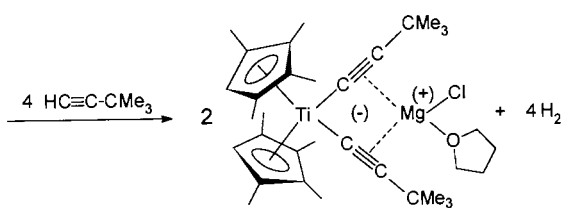

4

the bridging hydrogen atoms of **2** are replaced by bridging acetylide ligands with liberation of hydrogen. The valency of Ti (Ti(III)), the Mg–Cl bonds, and the coordination of THF to Mg remain unchanged. The dissociation of bridging Mg–Cl–Mg bonds is induced by a higher electron density flow to Mg from anionic acetylide ligands than from electron-deficient two-electron three-centered hydride bonds. Since compound **4** is coordinatively saturated it has only to be considered a catalytic precursor. Its dissociation affording $(\eta^5\text{-}C_5HMe_4)_2Ti(\eta^1\text{-}C{\equiv}CCMe_3)$,

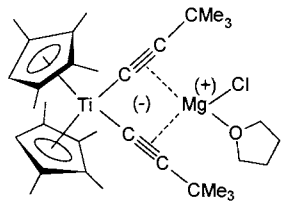

4

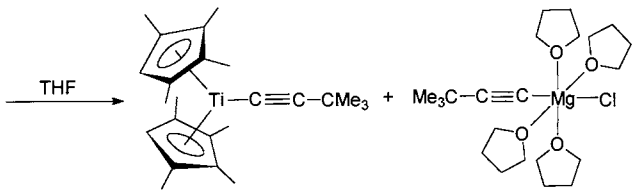

which probably displays the ESR signal **B** at $g = 1.951$ (Fig. 1(c)), must be a subsequent inevitable step. The clue role of this particle is corroborated by observations that the dimerization proceeds long after all **4** has disappeared and as long as a trace of the signal **B** is observable (in addition to the spectra of deactivation products). The dimerization may proceed either on the monomeric titanocene acetylide by the mechanism involving addition of TBUA to the acetylide and the elimination of HTTD by hydrogen transfer from a coordinating TBUA [2,6,8,22] or a change of valency to Ti(II) has to be assumed and a cycle involving the redox alternation between Ti(II) and Ti(IV) species can be suggested [28]. Neither of these alternatives can be approved by the present results. The occurrence of **6** as a product of deactivation by *tert*-butanol can be brought about by the ligand exchange between **5** and $MgCl_2$,

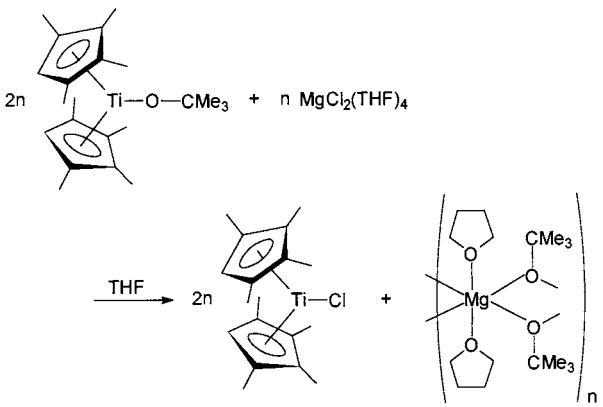

which is present in the system from the initial reduction of **1**. Since both **5** and **6** are monomeric, a polymeric di-*tert*-butoxymagnesium can lower the overall energy of the system.

3.4. Crystal structure of *2*

An ORTEP drawing of **2** and atom numbering scheme is shown in Fig. 2. Molecule **2** is a centrosymmetric dimer with magnesium atoms bonded by two

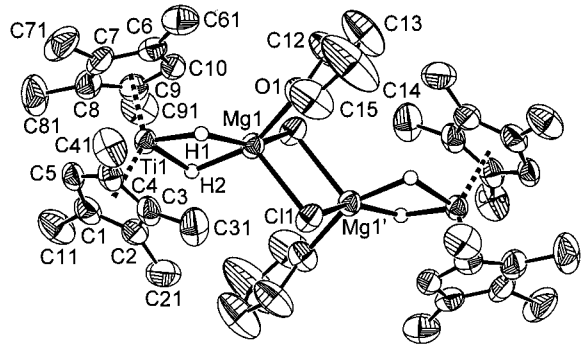

Fig. 2. ORTEP drawing of **2** with 30% probability ellipsoids and atom numbering scheme.

bridging chlorine atoms. Each titanium atom is coordinated by two η^5-C_5HMe_4 ligands and by two bridging hydrogen atoms binding the respective magnesium atom. Each magnesium atom coordinates one molecule of THF, thus reaching the coordination number five. Selected bond lengths and bond angles are listed in Table 2. All bonding distances and the structure of titanocene moieties are very similar to those of analogous diethyl ether-containing complex $[(\eta^5\text{-}C_5HMe_4)_2Ti(\mu\text{-}H)_2Mg(OEt_2)(\mu\text{-}Cl)]_2$ (**2′**) [18], differing noticeably in a larger CE(1)–Ti–CE(2) (CE-centroid of the cyclopentadienyl ring) angle (**2**, 141.4 vs. **2′**, 138.3°). The bridging fragments and the overall structure of **2**, however, differ from those of **2′**, apparently as a result of stronger electron donor ability of THF [28]. The different appearance of both the molecules is seen from Fig. 3. Whereas **2′** contains in addition to center of inversion an approximate molecular plane involving all metals, oxygen and centroids of cyclopentadienyl rings,

Table 2
Selected interatomic distances (A) and angles (°) for **2**

Interatomic distances (Å)			
Ti(1)–CE(1)	2.048(5)	Ti(1)–CE(2)	2.067(5)
Ti(1)–H(1)	1.711(42)	Ti(1)–H(2)	1.858(40)
Mg(1)–H(1)	1.987(42)	Mg(1)–H(2)	1.839(41)
Ti(1)–C(1)	2.361(4)	Ti(1)–C(2)	2.418(5)
Ti(1)–C(3)	2.417(4)	Ti(1)–C(4)	2.350(4)
Ti(1)–C(5)	2.311(4)	Ti(1)–C(6)	2.402(4)
Ti(1)–C(7)	2.415(5)	Ti(1)–C(8)	2.411(5)
Ti(1)–C(9)	2.382(4)	Ti(1)–C(10)	2.344(4)
Cl(1)–Mg(1)	2.4354(17)	Cl(1)–Mg(1)'	2.4545(16)
C_{ring}–$C_{ring,\ av.}$	1.410(7)	C_{ring}–$C_{Me,\ av.}$	1.505(7)
Ti(1)–Mg(1)	2.8492(15)	Mg(1)–Mg(1)′	3.440(3)
Angles (°)			
CE(1)–Ti(1)–CE(2)	141.4(2)	H(1)–Ti(1)–H(2)	79.7(19)
H(1)–Mg(1)–H(2)	73.4(18)	Ti(1)–H(1)–Mg(1)	100.5(20)
Ti(1)–H(2)–Mg(1)	100.8(19)	H(1)–Mg(1)–Cl(1)	113.9(12)
H(1)–Mg(1)–Cl(1)′	155.3(12)	H(2)–Mg(1)–Cl(1)	107.0(13)
H(2)–Mg(1)–Cl(1)′	96.8(13)	Mg(1)–Cl(1)–Mg(1)′	89.43(6)
Cl(1)–Mg(1)–Cl(1)′	90.57(6)	O(1)–Mg(1)–Cl(1)′	92.45(10)
O(1)–Mg(1)–Cl(1)	95.64(11)	O(1)–Mg(1)–H(1)	88.8(12)
O(1)–Mg(1)–H(2)	155.3(13)		

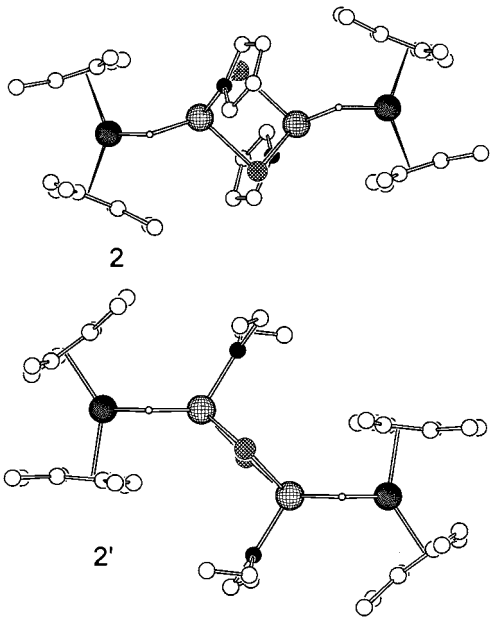

Fig. 3. View of PLUTON drawings of compounds **2** and **2′** in the direction perpendicular to CE(1), Ti, CE(2) planes.

compound **2** has no additional symmetry. In contrast to **2′**, the CE(1), Ti(1), CE(2) plane is not perpendicular to the Mg(1), Cl(1), Mg(1′), Cl(1′) plane. In **2**, the angle between these planes is 39.7°, and the Mg(1) atom is 0.043 Å and Cl(1) atom −0.106 Å away from the CE(1), Ti(1), CE(2) plane. Steric congestion between the CE(1) cyclopentadienyl ligand and this Cl(1) atom and/or THF ligand of the paired unit is responsible for folding of the hydrogen bridging plane. The dihedral angle between the Ti(1), H(1) and H(2) and Mg(1), H(1), H(2) planes is 22.6°. As a result of this distortion the least-squares planes of cyclopentadienyl rings CE(1) and CE(1′) are nearly parallel. The interconnections of Ti and Mg atoms in the chlorine-bridged units are parallel, shifted away towards the oxygen atoms of their THF ligands. The THF ligand is ca. planar and the Mg atom is 0.345 Å away from its least-squares plane. The Mg–O bond length of 2.062(3) Å falls into the range of bond lengths in reviewed structures with Mg–O bonds [29].

3.5. Crystal structure of *5*

An ORTEP drawing of **5** and atom numbering scheme is shown in Fig. 4. Selected bond distances and bond angles are listed in Table 3. The titanium atom is trigonally coordinated by two η^5-C_5HMe_4 ligands and by one *tert*-butoxy group. The CE(1), Ti(1), CE(2) plane is a molecular plane of symmetry which contains the O(1), C(12) and C(14) atoms of the *tert*-butoxy group; however, this symmetry plane is not manifested in crystal space group symmetry. Due to a low coordination number of titanium the bonds linking titanium are shorter than in similar tetrahedrally coordinated titanium compounds. Thus, the Ti–O bond length of 1.842(1) Å is shorter than Ti–O bonds in e.g. dimeric titanocene methoxide, $[(\eta^5\text{-}C_5H_5)_2Ti(\mu\text{-}OMe)]_2$ (2.065(2) Å) [30], acetylenedicarboxylate complex $[(\eta^5\text{-}C_5H_4Me)_2Ti]_2(O_2CC{\equiv}CCO_2)$ (1.96–1.97 Å) [31], bis(-benzoato) complex (1.92-1.93 A [32] or in titanocene carboxylates (2.13–2.17 Å) [33]. However, it is longer than the the Ti–O bonds in $(t\text{-}C_4H_9O)_3TiCo(CO)_3$ (av. 1.74 Å) [34]. The average Ti–CE distances in **5** (2.077 Å) are longer than this parameter in $(\eta^5\text{-}C_5HMe_4)_2TiCl$ (2.030 Å) [35]. This may reflect an extraordinary strength of a Ti–O bond. Some steric congestion due to the presence of the bulky *tert*-butoxy group is relieved by alternate orientation of the η^5-C_5HMe_4 ligands by the proton-bearing carbon atoms to the top of a hinge angle of cyclopentadienyl ligands (C(5)) and to the *tert*-butoxy side (C(10)). The bending of the Ti(1)–O(1)–C(12) bonds at the oxygen atom towards C(10) (162°) is, however, compensated by a larger O(1)–Ti(1)–CE(2) angle (115.0°) compared to O(1)–Ti(1)–CE(1) (108.4°).

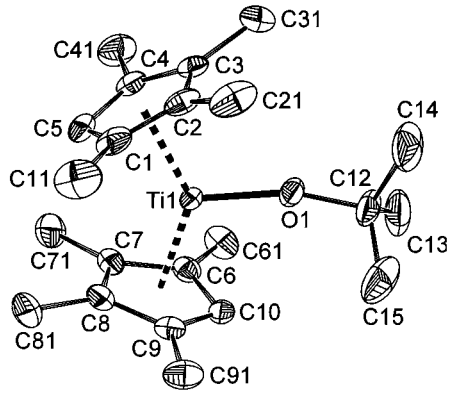

Fig. 4. ORTEP drawing of **5** with 30% probability ellipsoids and atom numbering scheme.

Table 3
Selected interatomic distances (A) and angles (°) for **5**

Bond distances (Å)			
Ti(1)–O(1)	1.8425(14)	Ti(1)–CE(1)	2.079(2)
Ti(1)–CE(2)	2.075(2)	Ti(1)–C(1)	2.384(2)
Ti(1)–C(2)	2.428(2)	Ti(1)–C(3)	2.428(2)
Ti(1)–C(4)	2.383(2)	Ti(1)–C(5)	2.380(2)
Ti(1)–C(6)	2.3740(19)	Ti(1)–C(7)	2.4528(19)
Ti(1)–C(8)	2.4478(19)	Ti(1)–C(9)	2.372(2)
Ti(1)–C(10)	2.341(2)	O(1)–C(12)	1.415(3)
C_{ring}–$C_{ring,\ av.}$	1.412(3)	C_{ring}–$C_{Me,\ av.}$	1.501(3)
Bond angles (°)			
O(1)–Ti(1)–CE(1)	108.4(1)	O(1)–Ti(1)–CE(2)	115.0(1)
CE(1)–Ti(1)–CE(2)	136.7(1)	C(12)–O(1)–Ti(1)	162.16(13)

4. Conclusions

Present results show that the selectivity of dimerization of terminal acetylenes can be controlled not only by a metal size but also, in the case of titanium, by steric congestion and/or electron density at the metal, both induced by substituents at the cyclopentadienyl ligands. In contrast to most other catalytic systems, the titanocene catalysts seem to act on an exclusion principle, catalyzing the head-to-tail dimerization of all current non-polar terminal acetylenes by decamethyltitanocene catalysts [2,3] and *tert*-butylacetylene by octamethyltitanocene ones. Intimate insight into the mechanism of HTTD formation is precluded by a low concentration of the catalytic complex as indicated by high concentrations of precursors **3** or **4** at high concentrations of TBUA and probably by a high activation energy required to introduce the catalytic complex, probably $(\eta^5\text{-}C_5HMe_4)_2Ti(\eta^1\text{-}C{\equiv}CCMe_3)$ into a catalytic cycle. Since the titanocene(Ti(II)-acetylene complexes are also well established precursors of head-to-tail dimerization of terminal acetylenes [28], investigations into the reasons for the revealed ligand-controlled selectivity should also run that line. In the case of TBUA, the presence of a catalyst-poisoning impurity must be eliminated. Only then, detailed kinetic measurements and investigation of reactions of a catalytic cycle can be performed.

5. Supplementary material available

Listings of atomic coordinates, bond lengths and angles and thermal parameters for **2** and **5** have been deposited at the Cambridge Crystallographic Data Centre. These, together with lists of observed and calculated structure factors and further details of the structure determination, are available from the authors (I. Císařová or M. Horáček).

Acknowledgements

This investigation was supported by the Grant Agency of Academy of Sciences of the Czech Republic (grant no. A4040711) and by the Grant Agency of the Czech Republic (grant no. 203/97/0242). The Grant Agency of the Czech Republic also sponsored (grant no. 203/96/0111) an access to Cambridge Structure Data Base. The authors are grateful to Petr Sedmera (Institute of Microbiology of Academy of Sciences, Prague) for NMR measurements.

References

[1] R. Anwander, in: B. Cornils, W.A. Herrmann (Eds.), Applied Homogeneous Catalysis with Organometallic Compounds, VCH Verlaggesellschaft mbH, Weinheim, FRG, 1996, Ch. 3.2.5, p. 876.
[2] M. Akita, H. Yasuda, A. Nakamura, Bull. Chem. Soc. Jpn. 57 (1984) 480.
[3] V. Varga, L. Petrusová, J. Čejka, K. Mach, J. Organomet. Chem. 532 (1997) 251.
[4] M.E. Thompson, S.M. Baxter, A.R. Bulls, B.J. Burger, M.C. Nolan, B.D. Santarsiero, W.P. Schaefer, J.E. Bercaw, J. Am. Chem. Soc. 109 (1987) 203.
[5] K.H. den Haan, Y. Wielstra, J.H. Teuben, Organometallics 6 (1987) 2053.
[6] H.J. Heeres, J.H. Teuben, Organometallics 10 (1991) 1980.
[7] H.J. Heeres, J. Nijhoff, J.H. Teuben, R.D. Rogers, Organometallics 12 (1993) 2609.
[8] A.D. Horton, J. Chem. Soc. Chem. Commun. (1992) 185.
[9] R.C. Weast (Editor-in-Chief), Handbook of Chemistry and Physics, 66th ed., CRC Press, Boca Raton, FL, USA, 1985–1986, table F-164.
[10] H. Antropiusová, A. Dosedlová, V. Hanuš, K. Mach, Transit. Met. Chem. 6 (1981) 90.
[11] S.I. Troyanov, V. Varga and K. Mach, J. Chem. Soc. Chem. Commun. (1993) 1174.
[12] K. Mach, V. Varga, H. Antropiusová, J. Poláček, J. Organomet. Chem. 333 (1987) 205.
[13] R. Gyepes, K. Mach, I. Císařová, J. Loub, J. Hiller, P. Šindelář, J. Organomet. Chem. 497 (1995) 33.
[14] S.I. Troyanov, V. Varga, K. Mach, Organometallics 12 (1993) 2820.
[15] K. Mach, J.B. Raynor, J. Chem. Soc. Faraday Trans. (1992) 683.
[16] G.M. Sheldrick, Acta Crystallogr. A46 (1990) 467.
[17] G.M. Sheldrick, SHELXL97. Program for the refinement of crystal structures. University of Göttingen, Göttingen 1997.
[18] S.I. Troyanov, V. Varga, K. Mach, J. Organomet. Chem. 461 (1993) 85.
[19] J.W. Pattiasina, H.J. Heeres, F. van Bolhuis, A. Meetsma, J.H. Teuben, A.L. Spek, Organometallics 6 (1987) 1004.
[20] W.W. Lukens, M.R. Smith III, R.A. Andersen, J. Am. Chem. Soc. 118 (1996) 1719.
[21] R. Gyepes, P. Štěpnička, U. Thewalt, M. Polášek, J. Čejka, M. Horáček, K. Mach, Collect. Czech. Chem. Commun. 63 (1998) 1884.
[22] M. Yoshida, R.F. Jordan, Organometallics 16 (1997) 4508.
[23] V. Varga, J. Hiller, M. Polášek, U. Thewalt, K. Mach, J. Organomet. Chem. 515 (1996) 57.
[24] J. Hiller, V. Varga, U. Thewalt, K. Mach, Collect. Czech. Chem. Commun. 62 (1997) 1446.
[25] (a) S. Back, H. Pritzkow, H. Lang, Organometallics, 17 (1998) 41. (b) M.D. Janssen, K. Köhler, M. Herres, A. Dedieu, W.J.J. Smeets, A.L. Spek, D.M. Grove, H. Lang, G. van Koten, J. Am. Chem. Soc. 118 (1996) 4817. (c) H. Lang, I.-Y. Wu, S. Weinmann, C. Weber, B. Nuber, J. Organomet. Chem. 541 (1997) 157. (d) H. Lang, S. Blau, B. Nuber, L. Zsolnai, Organometallics 14 (1995) 3216.
[26] J.M. de Wolf, R. Blaauw, A. Meetsma, J.H. Teuben, R. Gyepes, V. Varga, K. Mach, N. Veldman, A.L. Spek, Organometallics 15 (1996) 4977.
[27] G.A. Luinstra, L.C. ten Cate, H.J. Heeres, J.W. Pattiasina, A. Meetsma, J.H. Teuben, Organometallics 10 (1991) 3227.
[28] V. Varga, L. Petrusová, J. Čejka, V. Hanuš, K. Mach, J. Organomet. Chem. 509 (1996) 235.
[29] P.R. Markies, O.S. Akkerman, F. Bickelhaupt, W.J.J. Smeets, A.L. Spek, Adv. Organomet. Chem. 32 (1991) 147.
[30] E. Samuel, J.F. Harrod, D. Gourier, Y. Dromzee, F. Robert, Y. Jeannin, Inorg. Chem. 31 (1992) 3252.
[31] D.R. Corbin, J.L. Atwood, G.D. Stucky, Inorg. Chem. 25 (1986) 98.

[32] D.M. Hoffman, N.D. Chester, R.C. Fay, Organometallics 2 (1983) 48.
[33] A.W. Clauss, S.R. Wilson, R.M. Buchanan, C.G. Pierpont, D.N. Hendrickson, Inorg. Chem. 22 (1983) 628.
[34] D. Selent, R. Beckhaus, J. Pickhardt, Organometallics 12 (1993) 2857.
[35] S.I. Troyanov, V. Varga, K. Mach, J. Organomet. Chem. 461 (1993) 85.